Scientific African 31 (2026) e03255

Contents lists available at ScienceDirect

Scientific African

journal homepage: www.elsevier.com/locate/sciaf

Estimation of rainfall and wind impacts on fuel consumption of passenger vehicles: A physical model approach

Janet Appiah Osei [a,*], Rabani Adamou [a], Amos T. Kabo-Bah [b], Satyanarayana Narra [c], Konin Pierre-Claver Kakou [a]

[a] WASCAL Climate Change and Energy, Abdou Moumouni University, Niamey, Niger
[b] University of Energy and Natural Resources, Sunyani, Ghana
[c] West African Science Service Centre on Climate Change and Adapted Land Use (WASCAL), University of Lomé, Lomé, Togo

ARTICLE INFO

Editor: DR B Gyampoh

Keywords:
CO_2 emissions
Sustainable transport
Weather factors
Modeling and simulation

ABSTRACT

With the continuous changes in climate, increased attention is required to address the adverse impacts of climatic variables on automobile fuel consumption and emissions. In recent studies, various prediction models have been employed to quantify the influence of weather-related factors on vehicular fuel consumption. The paper introduces three interrelated vehicle-based physical models designed to quantify the effects of rainfall and wind speed/direction on fuel consumption of four commercial vehicles - Matiz, Astra, Pregio, and Urvan, utilizing monthly weather data from Accra. The results indicated that the presence of headwind and rainfall substantially increased fuel consumption, whereas tailwind contributed to a reduction. Fuel increments under rainfall and headwind ranged from 2 % to 10 % and 4 % to 16 %, respectively across the vehicles, depending on the monthly variation in weather intensity. Conversely, the reduction in fuel consumption due to tailwind ranged between 1 % and 3 %, insufficient to counteract the more significant increases induced by headwind. The combined impact of rainfall and wind increased fuel consumption by 10 % to 37 % relative to the effect of rainfall alone and by 5 % to 66 % compared to headwind effects, depending on monthly intensity levels. The proposed models demonstrated robust performance in analyzing weather-induced fuel consumption and can be effectively applied to estimate offline vehicular fuel usage prior to a journey.

Introduction

The urban population in Ghana has augmented rapidly since the mid-1900s. The proportion of the population residing in cities has increased significantly over the years, from 9 % in 1931 to 31.3 % in 1984, and finally to 43.8 % in 2000. Accra is a cardinal city in Ghana and the most urbanized, due to primacy in political, economic and cultural structures [1,2]. The city experiences a population growth rate of 4.2 % per year, surpassing the national growth rate of 2.7 % [3]. The rapid urbanization has led to a corresponding exponential rise in carbon dioxide (CO_2) emissions, significantly increasing the city's vulnerability to climate change impacts, which are evident in the recent shifts in rainfall and wind patterns [4–6]. The erratic weather conditions viciously affect fuel efficiency, as even slight fluctuations can produce significant impacts on fuel consumption [7].

Fuel consumption is influenced by several factors, which are broadly categorized into six main groups: vehicle, travel, traffic,

* Corresponding author.
E-mail address: janetoseiappiah@gmail.com (J.A. Osei).

https://doi.org/10.1016/j.sciaf.2026.e03255

Available online 12 February 2026

driver, road, and weather-related factors, with further sub-categorization summarized in Fig. 1 [8]. Among the categories, weather is the least studied factor [9,10]. In Accra, plethora of fuel consumption and emissions studies focus predominantly on traffic congestion, travel time and trips, driving style and road gradient with minimal attention given to weather factors [11–13]. Hitherto, no empirical data has been identified that explicitly examines the influence of weather variables on fuel consumption in Accra, to the authors' knowledge. The present study addresses the critical gap by providing the first empirical assessment of the effects of weather on vehicular fuel consumption and associated emissions in Ghana. Understanding such effects is crucial for estimating transport fuel costs and air pollution, thereby informing the development of short-, medium-, and long-term transport planning strategies that consider climate variability [14,15].

Existing literature on weather-related fuel consumption explicitly reveals the acute and chronic impacts of climate factors on road transportation. According to [16], key weather elements such as temperature, relative humidity, wind, rainfall and air pressure play significant and independent roles in reducing fuel efficiency and increasing on-road emissions. Hence, understanding the specific risks posed by each weather factor is essential for road transport development [17]. Rainfall and wind, in particular, have been empirically identified as significant contributors to increased fuel consumption and emissions among the other factors [18]. The associated impacts are primarily transmitted through changes in the resistance forces acting on a moving vehicle, especially aerodynamic drag [19]. Aerodynamic drag accounts for more than 50 % of a car's total energy consumption during motion, making drag a key determinant in vehicular fuel usage and emissions [20,21]. Consequently, the application of fuel consumption models is critical for quantifying the extent to which weather conditions affect fuel use and emissions. Real-world fuel consumption analysis is characterized by significant complexities, thereby increasing reliance on modelling and simulation tools. Such tools play fundamental roles in evaluating the environmental impacts of road transport and guiding the advancement of cleaner transport technologies [22].

Fuel consumption models are broadly categorized into two types: physical prediction models, which are grounded in vehicle dynamics, and data-driven prediction models. Data-driven models include Neural network models such as backpropagation neural networks, multilayer perceptron networks, long short-term memory (LSTM) networks as well as traditional machine learning algorithms like regression, random forest, decision tree and support vector machine [23]. Data-driven models are often hindered by construction complexity, limiting adoption within engineering applications [24]. Physical models, by contrast, offer reduced complexity and thus, broader applicability. Such models are constructed using mathematical formulas derived from internal vehicle structure and functional principles of the components. The flexibility of physical models allows for modifications based on specific research interest and available input data [25]. Numerous studies have validated the transparency and accuracy of physical models for fuel consumption estimation. For example, [26] reported a mean absolute percentage error (MAPE) of only 5 % in fuel consumption prediction using a physical model. Nonetheless, the application scope of physical models is often constrained by the seldom inclusion of weather-related variables [24]. Although some studies have included temperature and wind, weather elements are rarely the central focus. The integration of rainfall and wind effects into physical models remains inadequately explored in the literature. To address the identified research gap, a physical model emphasizing on rainfall and wind was developed to assess the impact of weather on vehicular fuel consumption and CO_2 emissions in Accra.

Materials and method

Case study in Accra

Accra, the capital of the Greater Accra Region, has an estimated population of 2,291,352, accounting for more than half of the

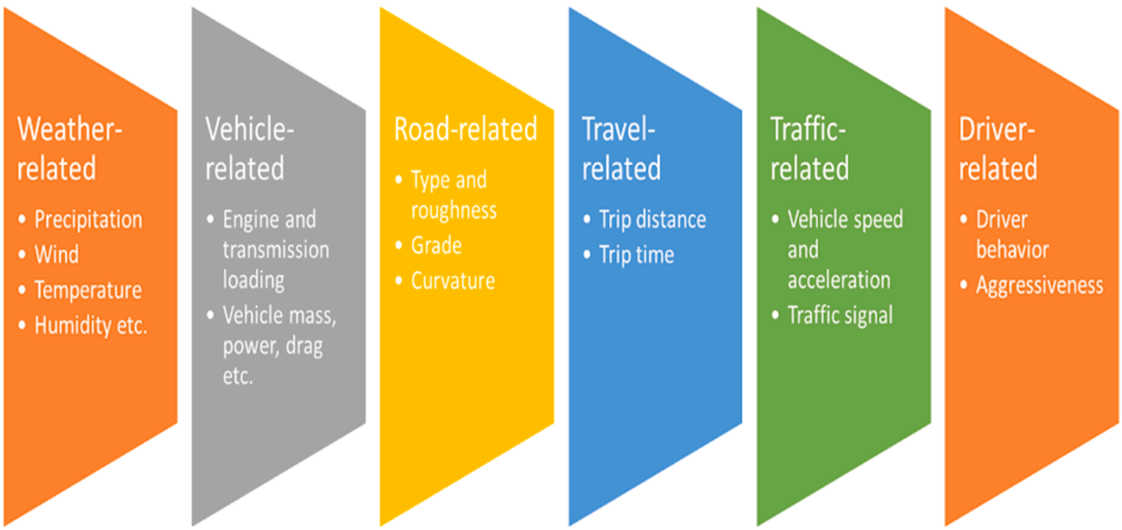

Fig. 1. Factors affecting vehicle fuel consumption.

region's total population. Driven by the exponential population growth, Accra is recognized as one of Africa's fastest-growing metropolises [27]. Accra lies within latitude 5°33′N and longitude 0°15′W, and is bordered to the north by Ga West Municipal, to the south by the Gulf of Guinea, to the west by Ga South Municipal, and to the east by La Dadekotopon Municipal. The city's terrain comprises lowlands and hills, with an average elevation ranging between 20-70 meters above mean sea level [28,29]. Fig. 2 presents an overview of Accra, highlighting the various towns, surrounding districts, and the existing road network.

Data source

Weather data used for model development was obtained from the Ghana Meteorological Agency. Fig. 3 displays the monthly average rainfall and wind speed from January to December. Vehicle selection for algorithm development focused on the most prevalent commercial passenger vehicles within Accra, identified through field observation. Four predominant vehicle types were used: two minibuses -trotro (Pregio and Urvan) and two taxis - Matiz and Astra. Technical specifications of the vehicles based on manufacturer documentation are presented in Table 1.

Modelling and simulation process

Model development

The initial stage in the development of a physical model involves identification of the physical system and selection of key components relevant to the modeling process, while disregarding non-essential elements. The subsequent stage entails the formulation of mathematical Eq.s that represent the dynamics and interactions of the selected components. The resulting model is then simulated using appropriate computational tools to generate outputs that describe the system's behavior in detail. Finally, a validation process is conducted to assess the accuracy of the simulated results in representing the actual physical system [30]. The overall structure of a typical physical model design is illustrated in Fig. 4.

In accordance with the framework outlined in Fig. 4, the specifications of the selected vehicles, as detailed in Table 1 were integrated into the modelling process. The vehicle system was mathematized through the development of algorithms based on the three primary resistance forces experienced during vehicle motion: air resistance (aerodynamic drag), rolling resistance, and inertial acceleration, as displayed in Fig. 5 [31]. The algorithms were selected due to the efficacy in interrelating key variables, to enable accurate prediction of fuel consumption.

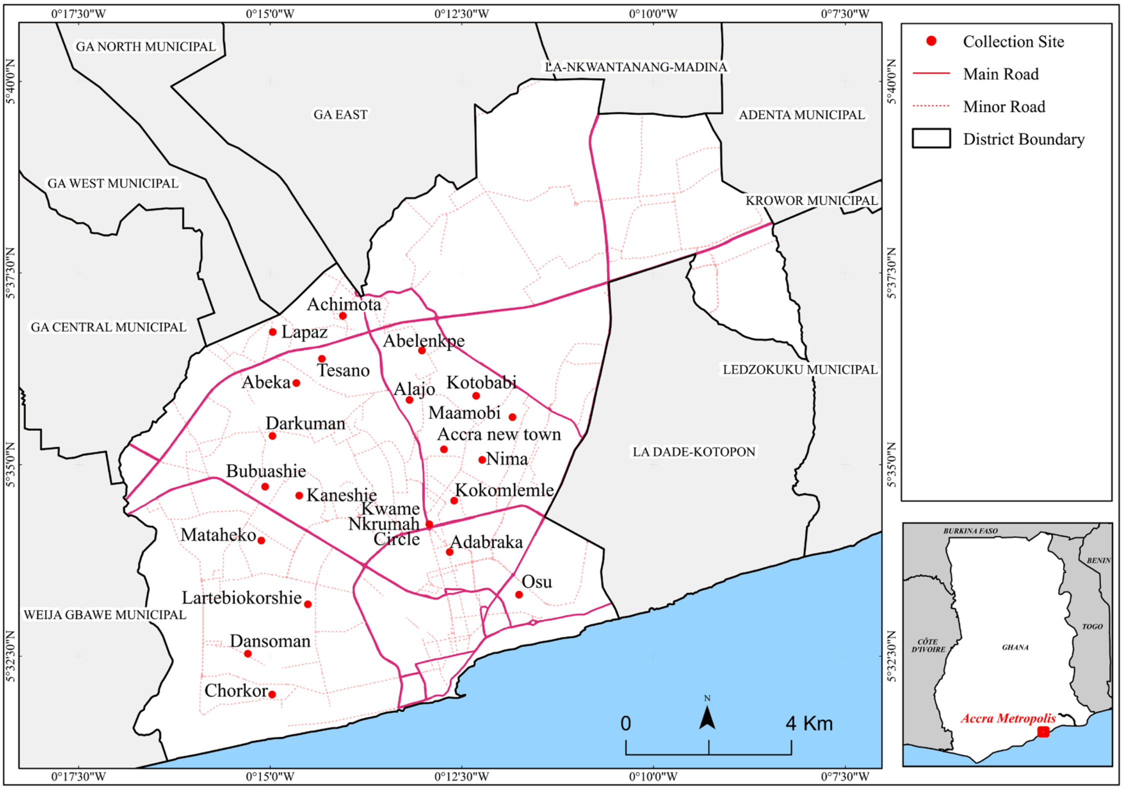

Fig. 2. Map of Accra metropolis.

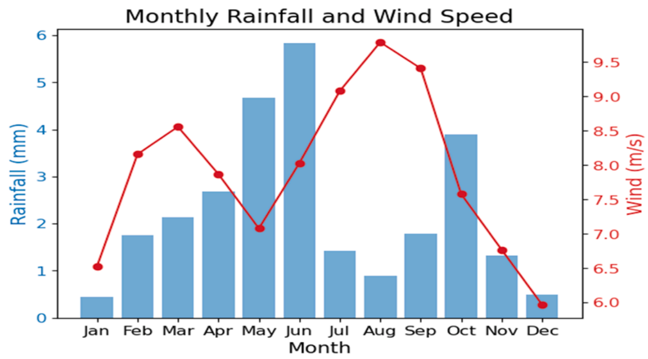

Fig. 3. Average wind speed and rainfall in Accra from January to December.

Table 1
Components of selected passenger vehicles.

Vehicle Make	Model	Mass (kg)	Frontal area (m^2)	Aerodynamic drag (kW)	Engine maximum power (kW)	Acceleration (m/s^2)
Chevrolet	Matiz	775	1.91	0.34	38	1.63
Opel	Astra	1165	2.06	0.32	77	2.26
Nissan	Urvan	1800	2.86	0.37	97	2.46
Kia	Pregio	1790	3.08	0.38	63	2.08

Definition of algorithmic forces

Rolling resistance force

Rolling resistance is the force that opposes the motion of a rolling body in contact with a surface. Approximately 90 % of the occurrence is attributed to material hysteresis, with the remainder resulting from friction losses and aerodynamic factors around the tire [32]. Eq. 1 defines the rolling resistance force of a moving vehicle.

$$F_{roll} = f\left\langle 1 + \frac{v}{147} \right\rangle mg \tag{1}$$

Aerodynamic drag

Aerodynamic drag refers to the resistance force exerted by air on a moving object. Additionally, drag denotes a fluid force acting on a solid body moving in the direction of the free-stream flow of the fluid [33]. Air drag results primarily from pressure drag and form drag, with pressure drag accounting for more than 80 % of the total aerodynamic force in vehicles [34]. The state-of the -art drag Eq. is expressed in Eq. 2.

$$F_{drag} = 0.5 * d * A * \rho a * v^2 \tag{2}$$

The general drag model was modified to account for rainfall and wind effects, in alignment with the approaches in [35,36]. The modification allowed for the integration of the terminal velocity of raindrops and longitudinal wind direction components (headwind

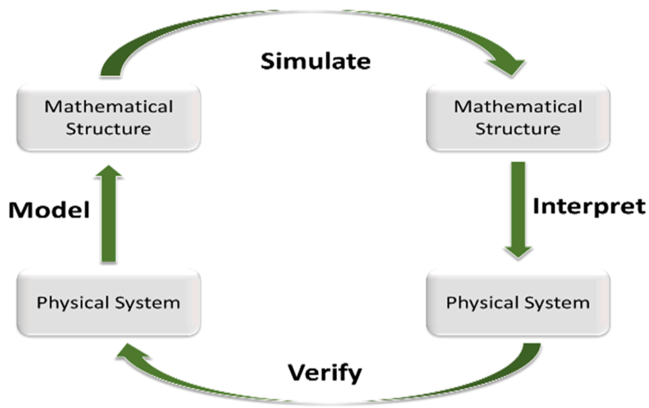

Fig. 4. Structure of a general physical model.

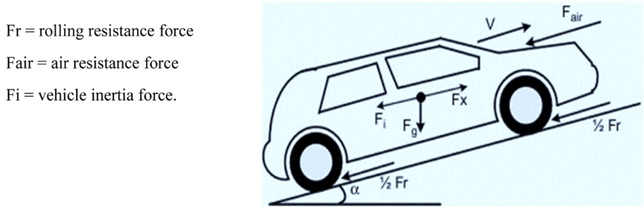

Fig. 5. A vehicle model displaying the three main resistance forces [31].

and tailwind) to enhance the applicability of drag model under varying weather conditions.

Force of inertia acceleration

Vehicles accelerate only when drivetrain provide sufficient energy to overcome inertia which is directly proportional to vehicle mass [37]. A vehicle in acceleration mode accelerates alongside the mass and rotating parts of the wheels [38]. Therefore, the power to overcome inertial acceleration is expressed using Eq. 3.

$$F_{inertia} = ma \tag{3}$$

Where: f = rolling resistance coefficient (0.025 for bitumen surface-treated roads) [37]; m= vehicle mass (kg); g=acceleration due to gravity (9.8 m/s); v= velocity in m/s; a= vehicle acceleration (m/s^2);

ρ_a= air density; d= vehicle aerodynamic drag coefficient (kW);

A= vehicle frontal area (m^2)

Definition of variables

The variables employed in the model were categorized into three main parts - target, main predictor and supporting predictor variables, as displayed in Fig. 6. Monthly rainfall and wind were designated as the main predictors, while speed (40 km/h), selected based on the recommended urban speed limit in Ghana, and road pavement (bitumen surface-treated) served as supporting predictors. Using the outlined variables, weather-defined fuel consumption models were further developed, as detailed in the subsections.

The approach introduces a novel methodology in physical vehicle-based modeling, which focuses solely on vehicle dynamics and often characterized as a single data dimension model [23], by incorporating and stressing on weather factors that are typically under-emphasized.

Rainfall model

According to [39], quantifying the effects of rainfall on fuel consumption is highly complex and thus, seldomly studied. Existing research primarily focuses on how rain impacts road surface and, consequently, fuel consumption. However, the influence of rain on fuel consumption via aerodynamics remains underexplored in literature [19,40]. The study applied the principle of terminal velocity, which describes the equilibrium velocity of a particle falling through still air, to quantify the aerodynamic impacts of rain on fuel consumption [41–43].

Six terminal velocity models [44–49], defined in Eq.s 4 to 9, were evaluated using sensitivity analysis on droplet diameters ranging

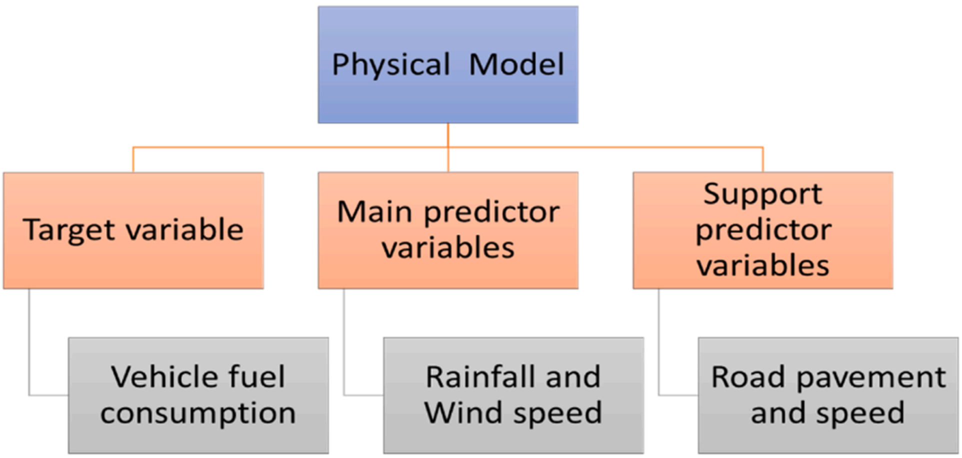

Fig. 6. Model framework defining the variables.

from 0.2 mm to 5 mm. The relationship between rainfall volume in Fig. 3, the corresponding droplet diameters and terminal velocities is illustrated in Fig. 10.

Best (1950) model

$$v_t = 958\left[1 - \exp\left(-\left(\frac{d}{0.171}\right)^{1.147}\right)\right] \tag{4}$$

Kessler (1969) model

$$v_t = 1300d^{0.5} \tag{5}$$

Atlas et al. (1973) model

$$v_t = 965 - 1030\exp(-6d) \tag{6}$$

Atlas & Ulbrich (1977) model

$$v_t = 1767d^{0.67} \tag{7}$$

Willis (1984) model

$$v_t = 4854d\ exp\ (-1.94d) \tag{8}$$

Brandes et al. (2002) model

$$v_t = \ -10.21 + 4932d - 9551d^2 + 7934d^3 - 2362d^4 \tag{9}$$

Where:

v_t = terminal velocity (cm/s); d = droplet diameter (cm)

Fig. 7 shows the performance of the evaluated models. The model proposed by Atlas & Ulbrich demonstrated superior linearity and achieved the highest R^2 value of 0.99, outperforming the other models, and was therefore selected as the optimal terminal velocity model for the study. Consequently, a novel mathematical algorithm for quantifying precipitation impacts on vehicle fuel consumption is presented in Eq. 10. Additionally, Eq. 11 denotes how fuel consumption changes with respect to the terminal velocity of raindrops. The model defines rainfall in the absence of wind, as illustrated in Fig. 8, where raindrops are depicted falling vertically.

$$Q\left(\frac{l}{100km}\right) = \frac{bsf * 10^{-2}(F_{roll} * F_{inertia} * \ [0.5.\ \mathrm{d}\ .\ \mathrm{A}.\ \rho\mathrm{a}.\ (\mathrm{v} + v_t)^3] * v^2)}{\eta\mathrm{T}.\ \rho\mathrm{f}.\ \mathrm{v}} + \left[1 + \frac{(v + v_t)^2}{\beta}\right] \tag{10}$$

Differentiating Q with respect to fall velocity:

$$\frac{\partial Q}{\partial v_t} = \frac{bsf * 10^{-2} * F_{roll} * F_{inertia} * (0.5.d.A.\rho\mathrm{a.v.}3(\mathrm{v} + v_t)^2)}{\eta\mathrm{T}.\rho\mathrm{f}} + \frac{2(v + v_t)}{\beta} \tag{11}$$

Where:

Bsf = brake specific fuel consumption taken as a constant,

ηT = transmission efficiency,

ρf = fuel density and

β = constant.

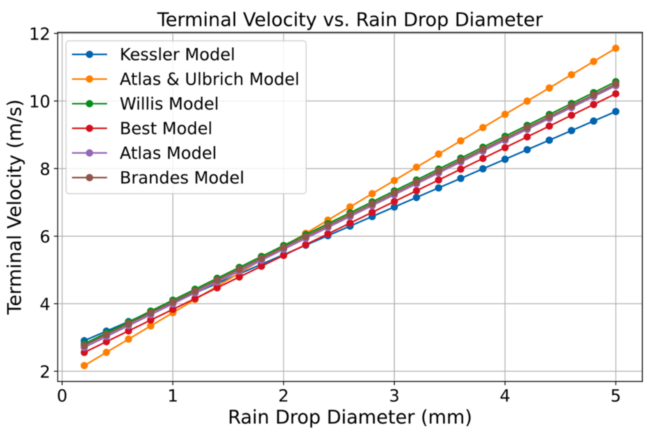

Fig. 7. Performance of terminal velocity models.

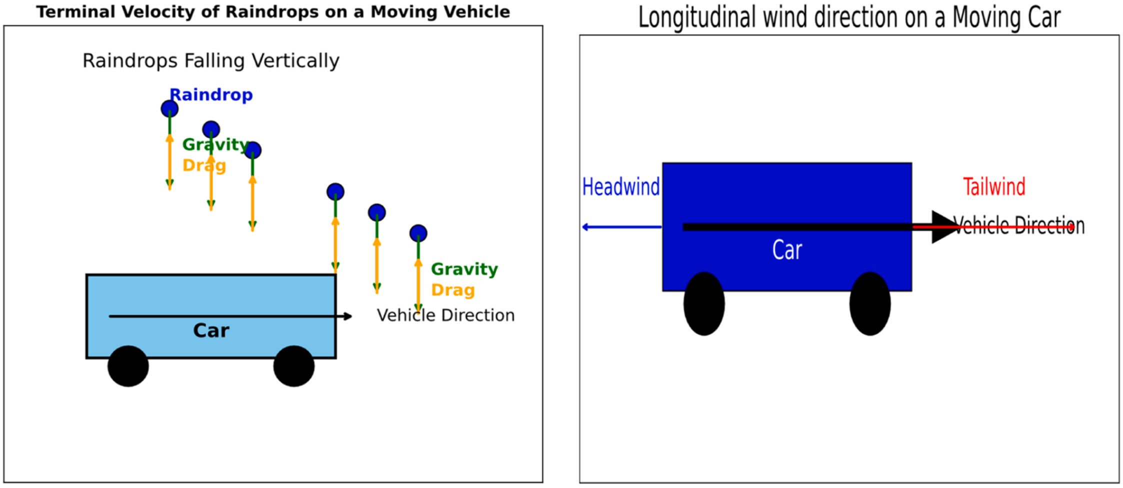

Fig. 8. Falling rain drops and wind direction of a vehicle in motion.

Wind model

The impact of wind on fuel consumption depends on both wind direction and speed [50]. Two directional categories were defined: headwind and tailwind, illustrated in Fig. 8. The wind effect was determined by applying Eq. 12, which incorporates cardinal directions.

$$W = ws.\cos\ (\mathrm{h}\ -\ (\phi +\ \mathrm{wd}) \tag{12}$$

Where;

W= wind effect; ws = wind speed (m/s); wd = wind direction

ф and h (rad) = directional angles of wind and vehicle movement, respectively

The proposed model to quantify the influence of wind on fuel consumption is presented in Eq. 13, while Eq. 14 describes the variation of fuel consumption with respect to wind effects.

$$\mathrm{Q}\left(\frac{l}{100km}\right) = \frac{bsf * 10^{-2}(F_{roll} * F_{inertia} * [0.5.\ \mathrm{d.\ A}\ .\rho \mathrm{a.}\ (\mathrm{v}-\mathrm{W})^{\ 3}] * v^2)}{\eta \mathrm{T}.\rho \mathrm{f.v}} + \left(1+\frac{(v-W)^2}{\beta}\right) \tag{13}$$

Differentiating Q with respect to wind effects:

$$\frac{\partial Q}{\partial \mathrm{W}} = \frac{bsf * 10^{-2} * F_{roll} * F_{inertia} * \left(0.5 * d.\ A.\rho \mathrm{a.\ v.} - 3\ [\mathrm{v}-\mathrm{W}]^2\right)}{\eta \mathrm{T}.\rho \mathrm{f}} - \frac{2(v-\mathrm{W})}{\beta} \tag{14}$$

Simulation environment

Simulations were run in python using SimPy - a process-based discrete-event simulation framework. SimPy was selected for its ability to model time-dependent processes through event scheduling, making it suitable for simulating the impact of monthly weather factors- specifically wind speed and rainfall on the fuel consumption of commercial vehicles. The simulations involved systematically varying individual monthly rainfall and wind inputs along with the vehicle specifications, while keeping speed and road pavement constant. To simulate rain-wind interactions, a compound model combining both effects was developed and is presented in Eq. 15, with Eq. 16 showing how fuel consumption fluctuates with respect to the combined influence of wind and the terminal velocity of raindrops.

$$\mathrm{Q}\ \left(\frac{l}{100km}\right) = \frac{bsf * 10^{-2}(F_{roll} * F_{inertia} * \ [0.5\ .\ \mathrm{d.\ A.}\ \rho \mathrm{a.}\ (\mathrm{v}-(\mathrm{W}+v_t))^{\ 3}]\ *\ v^2)}{\eta \mathrm{T}.\rho \mathrm{f.\ v}} + \left[1+\frac{[\mathrm{v}-(\mathrm{W}+v_t)]^2}{\beta}\right] \tag{15}$$

Differentiating Q with respect to fall velocity and wind effects:

$$\frac{\partial Q}{\partial\ (W+v_t)} = \frac{bsf * 10^{-2} * F_{roll} * F_{inertia} * [0.5.d.A.\rho \mathrm{a.v.} - 3(\mathrm{v}-(\mathrm{W}+v_t))]^2}{\eta \mathrm{T}.\rho \mathrm{f}} - \frac{2[\mathrm{v}-(\mathrm{W}+v_t)]}{\beta} \tag{16}$$

Simulation outputs, including detailed fuel consumption metrics under the specified conditions were collected, interpreted and validated. Fig. 9 describes how the proposed models were applied to simulate fuel consumption of the commercial vehicles.

Model validation

Field trials were carried out with three commercial vehicles - Chevrolet Matiz, Opel Astra, and Toyota HiAce along predefined routes in the Kwame Nkrumah Circle, Accra between September and October 2023, a period characterized by frequent rainfall. Ambient weather data were obtained from a nearby synoptic station. Fuel consumption was measured manually using dashboard readings. Prior to each trial, the fuel tank of each vehicle was filled to capacity, and final consumption was determined by refilling the tank and measuring the volume used. To isolate individual weather effects, observed fuel consumption data were recorded under the following conditions: consumption from runs with significant rainfall and negligible wind were recorded as rainfall-only; runs with both apparent wind and rainfall as combined conditions; and runs with substantial wind but no rainfall as wind-only. The observed values were then compared with the model-predicted values after data tuning to ensure each model accurately represented the corresponding weather factor.

Model performance was evaluated using R^2, Mean Absolute Error (MAE), and Mean Absolute Percentage Error (MAPE), as defined in Eq.s 17 to 22. R^2 values close to 1 indicate strong model accuracy, while MAE and MAPE measure actual and relative prediction errors, respectively [18,51,52].

$$\overline{\mathrm{Y}} = \frac{1}{n}\sum_{i=1}^{n} Yi \tag{17}$$

$$\mathrm{MST} = \frac{1}{n}\sum_{i=1}^{n} (Yi - \overline{\mathrm{Y}})^2 \tag{18}$$

$$\mathrm{MSE} = \frac{1}{n}\sum_{i=1}^{n} (Xi - \mathrm{Y}i)^2 \tag{19}$$

$$\mathrm{R}^2 = 1 - \frac{MSE}{MST} \tag{20}$$

$$\mathrm{MAE} = \frac{1}{n}\sum_{i=1}^{n} (Xi - \mathrm{Y}i) \tag{21}$$

$$\mathrm{MAPE} = \frac{1}{n}\sum_{i=1}^{n} \left[\frac{Xi - Yi}{Yi}\right] \tag{22}$$

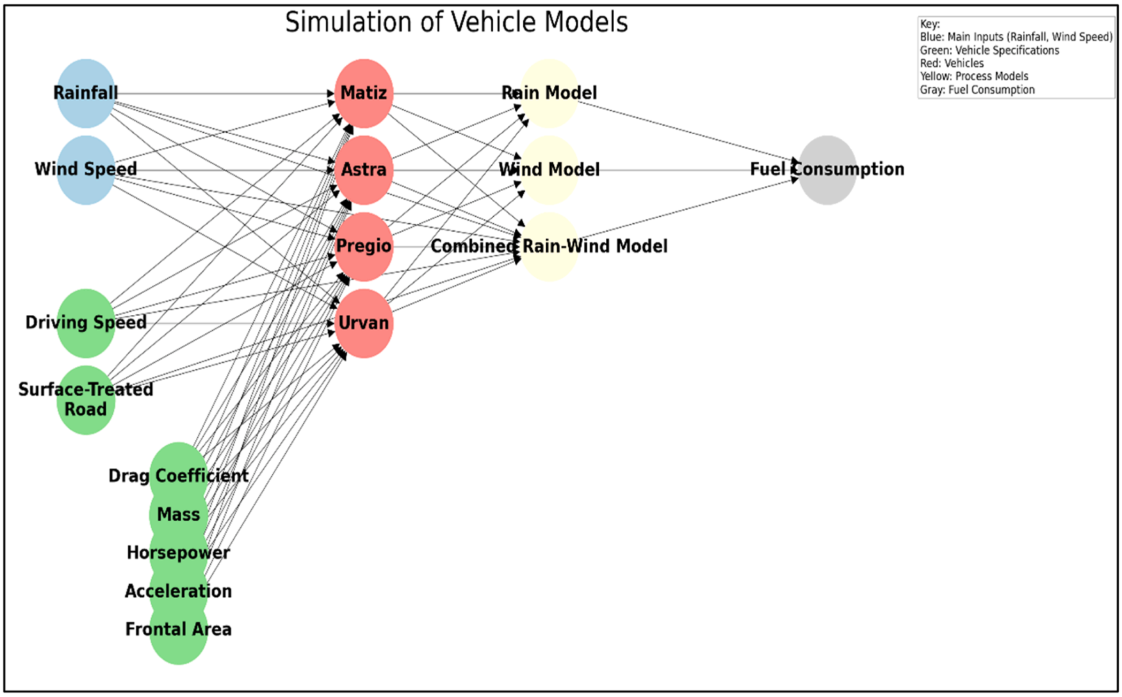

Fig. 9. Framework of simulation process.

Where:

Xi is the predicted ith value,

Yi is the observed ith value;

$\bar{Y}$ is the mean of the observed value;

MST is the mean total sum of squares; n is the number of predicted results.

In addition to the field experimentation, a sensitivity analysis was carried out using a one-factor-at-a-time variation approach to evaluate the influence of the weather factors on the model output. The analysis was interpreted using standardized regression coefficients (SRC), margin of error (MoE), confidence intervals (CI) and standard deviation (SD). All computations were carried out in a Jupyter Notebook environment using the Python programming language and custom-developed scripts.

Determination of carbon dioxide emissions

CO_2 emissions were estimated using the simulated outputs and the default emission factors outlined in the IPCC 2006 guidelines. The default values were employed due to the unavailability of country-specific emission factors for Ghana. Eq. 23 presents the computation for the tailpipe CO_2 emissions.

$$CO_2\ (\text{kg-}CO_2\text{eq}) = F_f \times EF_{CO2} \times GWP_{CO2} \tag{23}$$

Where:

F_f = predicted fuel consumption (TJ);

EF_{CO2} = emission factor given as 69300 (kg/TJ) and 74100 (kg/TJ) for gasoline and diesel respectively;

GWP is global warming potential given as 1 [53].

Results and discussion

The findings provide the first empirical evidence on the impact of rainfall and wind speed on commercial vehicle fuel consumption and emissions in Ghana. The novel methodological approach adopted proved effective in generating robust results, which are elaborated in the following subsections.

Rainfall and wind effects on aerodynamic drag

Weather variables influence vehicle aerodynamic drag which ultimately affect fuel consumption and emissions [19,21]. Determining aerodynamic drag requires quantifying the wind direction and terminal velocity of rain drops, as depicted in Fig. 10. A linear relationship was observed between rainfall and both raindrop diameter and terminal velocity. Specifically, a 1 mm increase in rainfall

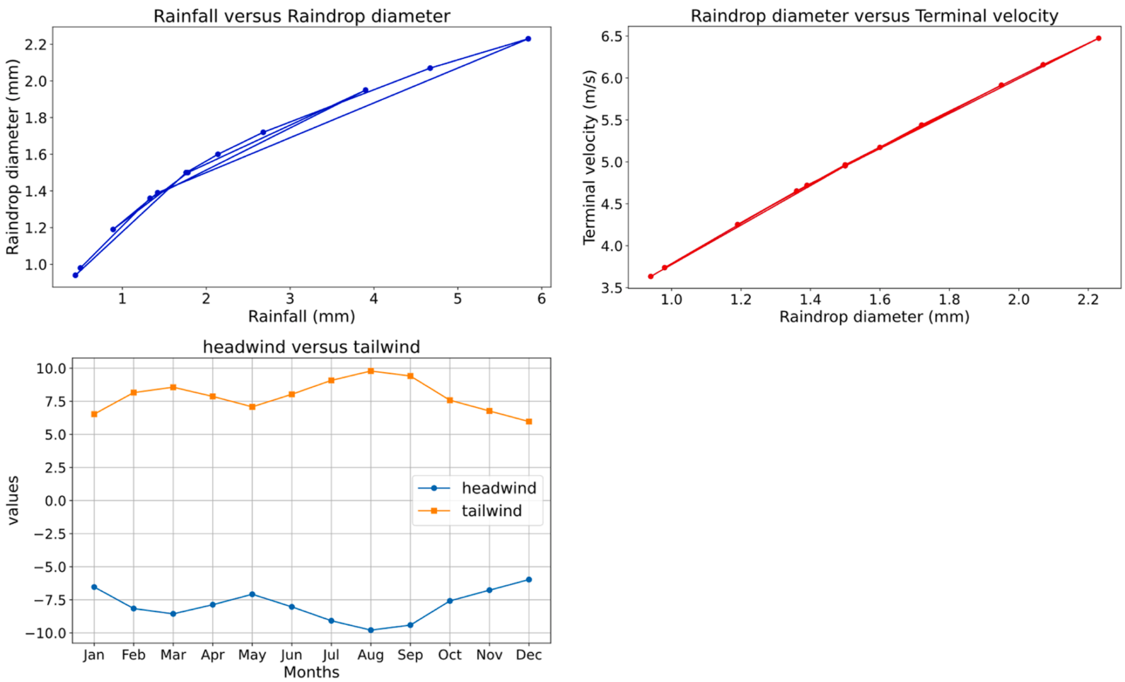

Fig. 10. Terminal velocity of rain drops alongside head and tail wind effects.

corresponded to a 0.197 mm rise in droplet diameter and a 0.413 m/s rise in terminal velocity. Droplet diameters below 1 mm exhibited fall speeds of less than 4 m/s, diameters ranging from 1 to 1.5 mm exhibited fall speeds between 4.3 and 5 m/s, and diameters between 1.6 and 2.5 mm exhibited fall speeds of 5.2 to 6.5 m/s. The findings align with [54], which reported an increase in raindrop size with rising rainfall intensities under controlled wind tunnel conditions.

The quantification of wind directions using cosine functions, as detailed in Eq. 12, defined tailwind and headwind effects as +1 and -1, respectively [55]. However, under vehicle aerodynamics, the tail side corresponds to a negative wind environment whilst head side represents positive wind conditions [50].

Consequently, the direct effects of the quantified wind and rainfall on aerodynamic drag of vehicles are illustrated in Fig. 11. The effects were ascertained through simulations comparing baseline conditions (excluding weather influences) with weather-affected scenarios. The results show that rainfall and headwind significantly increase aerodynamic drag, while tailwind causes a slight reduction in drag relative to the baseline (control). The intensity of the variables contributed significantly to the degree of aerodynamic drag experienced by the vehicles. Months characterized by higher rainfall and stronger wind speeds corresponded to greater aerodynamic drag and vice versa.

Peak rainfall in June contributed to a 360 % increase in aerodynamic drag compared with a 171.5 % rise in January, the month with the lowest rainfall. The remaining months exhibited a consistent incremental trend in aerodynamic drag corresponding to the rainfall values depicted in Fig. 3, with increases of 251 % in February, 265.7 % in March, 284 % in April, 336.2 % in May, 236 % in July, 207 % in August, 252 % in September, 318 % in October, 231.7 % in November, and 177.3 % in December compared to the control. Similarly, [56] observed a distinct increase in drag as rainfall increased from 8 mm/hr to 29 mm/hr [57]. reported elevated aerodynamic drag under heavier precipitation when quantifying precipitation effects on moving vehicles.

Peak wind conditions in August resulted in a 7.7-fold increase in aerodynamic drag, while wind speeds in the remaining months elevated drag by 4 to 7-folds under headwind conditions, depending on intensity. In contrast, tailwind reduced air drag by 80–99 % across all months. The observed trend aligns with the findings of [35] and [50], who reported similar changes in aerodynamic resistance based on wind direction and intensity.

The observed changes in aerodynamic drag under the influence of the weather factors are attributed to the phenomenon of streamline formation. In aerodynamics, streamlining describes air flowing in a definite pattern with a moving body. The presence of headwind and rainfall causes air disturbance and turbulence that disrupt streamlines. The greater the intensity, the more significant

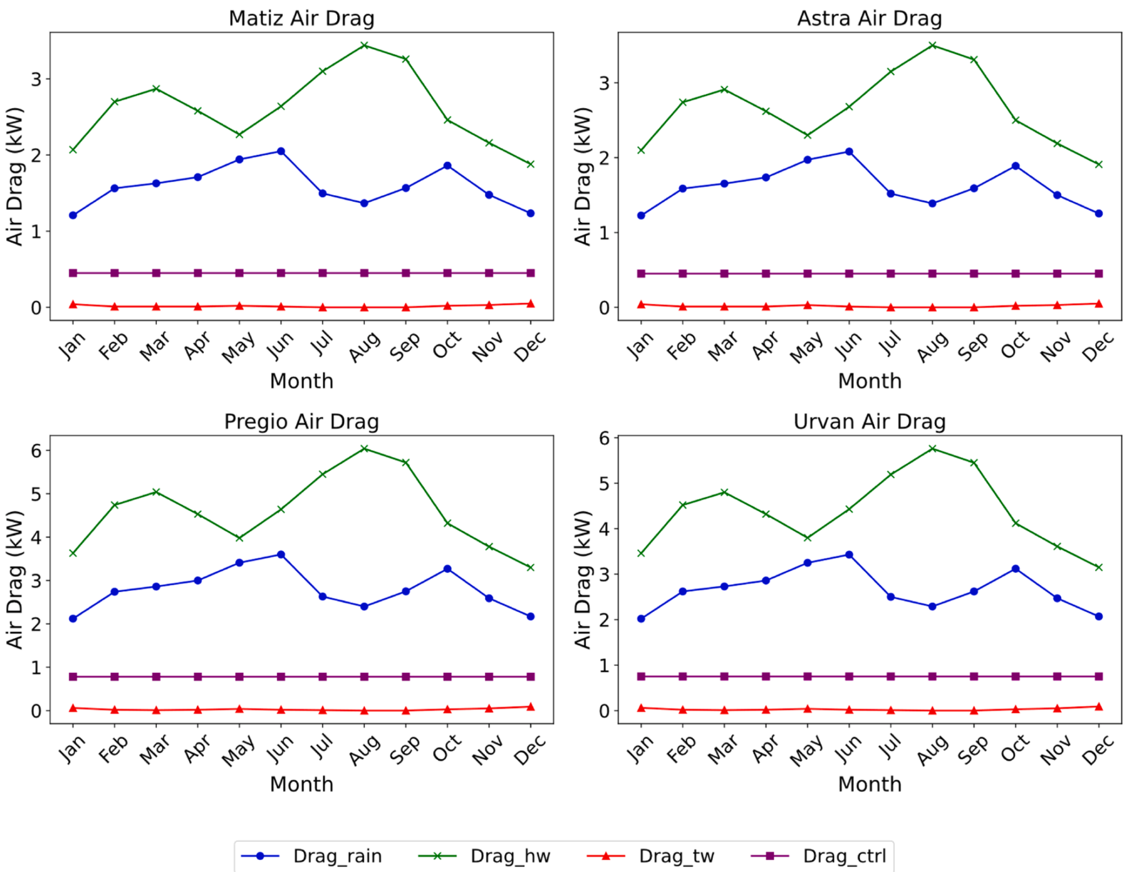

Fig. 11. Rainfall and wind impact on air drag of the vehicles.

the disruption and consequently, the higher the aerodynamic drag [58]. Conversely, tailwind conditions, promotes streamline alignment, reduces downstream turbulence and thus, lower aerodynamic drag [59,60].

Quantification of fuel consumption and CO_2 emissions

Building on the aerodynamic impacts described in section 3.1, the presented findings in section 3.2 quantify the resulting changes in fuel consumption and CO_2 emissions. Fig. 12 illustrates the fuel consumption and CO_2 emissions of the different vehicles under both the baseline (control) and weather-affected scenarios. Baseline fuel consumption and emissions were significantly lower than

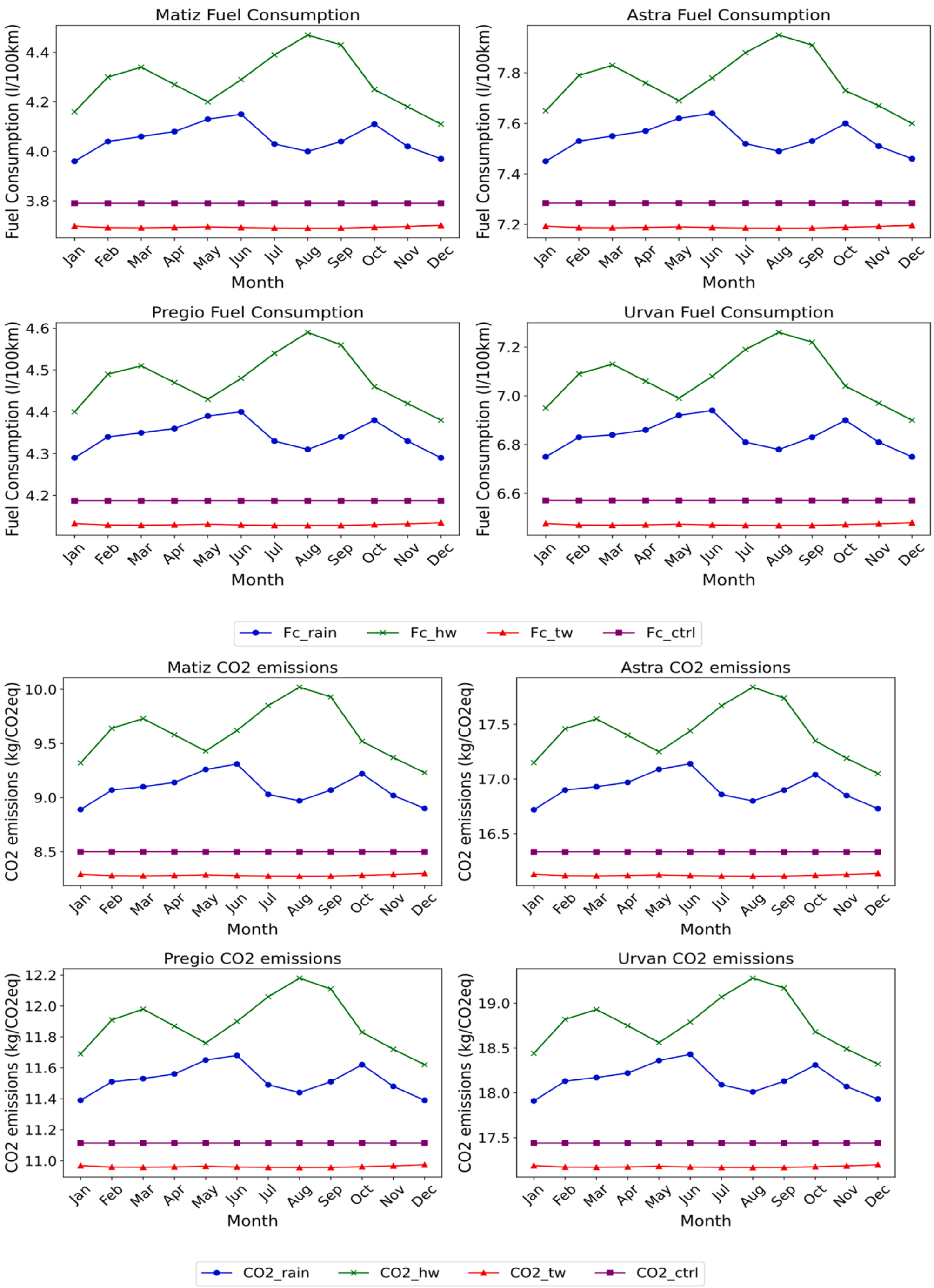

Fig. 12. Fuel consumption and CO_2 emissions under rainfall and wind conditions.

emissions observed under headwind and rainfall conditions, but slightly higher than emissions under tailwind environment. Thus, tailwind lowered fuel consumption and emissions, while headwind and rainfall led to increases, as depicted in Fig. 12. The trend is further illustrated in Fig. 13, which presents the percentage emission changes associated with each weather condition. The percentage CO_2 emissions increased substantially under headwind and rainfall, while a decrease was observed under tailwind conditions. However, the magnitude of the decrease associated with tailwind was insufficient to offset the significant increases caused by headwind. Therefore, under combined head- tailwind conditions, the net impact on fuel consumption and CO_2 emissions remains considerable. For instance, in February, the Matiz vehicle recorded a 13.45 % CO_2 increase under headwind and a 2.44 % decrease under tailwind, yielding a net increase of 11.01 %. The significant net increment highlights the dominant influence of longitudinal wind, despite the partial benefits from tailwind. The predominance of headwind effects is attributed to the additional energy demand imposed on a moving vehicle to counteract strong forces and neutralize the opposing wind [19]. Similarly, the study by [50] observed a 41 % increase in fuel consumption under headwind conditions, compared with only a 7.3 % decrease under tailwind. Studies by [61, 62] reported fuel savings under tailwind to be inadequate to counterbalance substantial increases caused by headwind.

The vehicles exhibited varying sensitivity to the impact of the weather conditions. As depicted in Fig. 13, Matiz recorded the highest percentage change in CO_2 emissions. The influence of the weather factors on Matiz's emissions was approximately twice that observed in the other vehicles, highlighting the greater susceptibility of lighter vehicles to the effects of rainfall and wind speed.

Impacts of vehicle types and specifications on fuel consumption and emissions

The different passenger vehicles exhibited distinct variations in fuel consumption and CO_2 emission rates, as illustrated in Fig. 12. Albeit Matiz displayed the greatest sensitivity to weather conditions, the model demonstrated the highest fuel efficiency. Relative to Astra, Matiz achieved fuel savings of 46.8 % under rainfall and 45.6 % under headwind. Within the trotro category, Pregio vehicle lowered emissions by 36 % under rainfall and 36.6 % under headwind compared with the Urvan. The observed variations underscore the significant influence of vehicle model specifications on fuel consumption and emission rates.

Vehicle specifications primarily affect fuel consumption rates through impacts on the three resistance forces encountered during motion [63]. Thus, the greater the value of the vehicle component, the higher the associated resistance force which ultimately, affect the rate of fuel consumption and emissions. Vehicle mass affects rolling resistance and inertia acceleration forces, engine maximum power impacts inertia acceleration, whilst drag coefficient and frontal area influence aerodynamic drag.

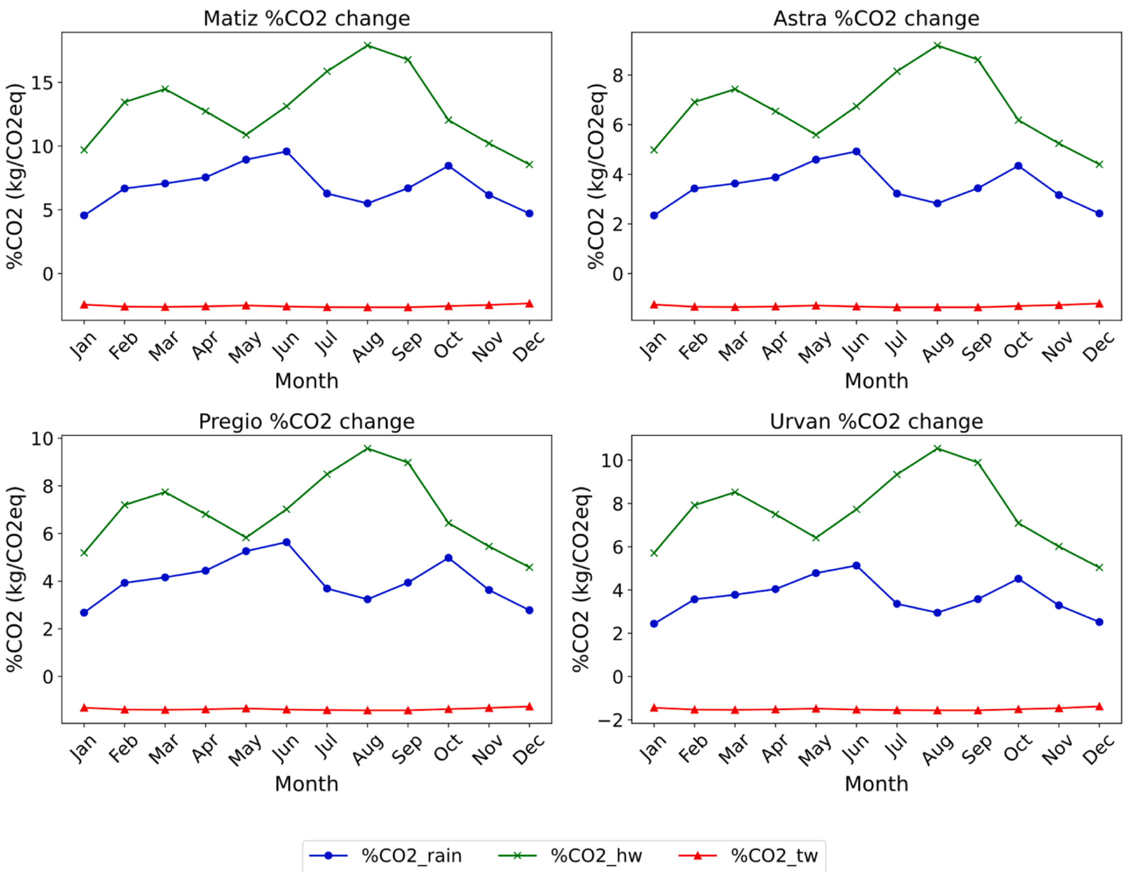

Fig. 13. Percentage CO_2 emissions under rainfall and wind speed.

Each specification contributes uniquely to overall fuel consumption, with individual factors potentially offsetting or outweighing one another, as clearly illustrated by the comparison between Pregio and Urvan. According to Table 1, Pregio exhibits a greater frontal area and higher drag coefficient, nevertheless, the Urvan demonstrates higher overall fuel consumption due to the larger mass and greater engine maximum power, which result in increased rolling resistance and inertial forces. Specifically, the rolling resistance and inertial acceleration forces of the Urvan were 0.99 times and 1.18 times greater than the Pregio's, respectively, thereby contributing substantially to the total fuel expenditure and emission rates, as observed in Fig. 12. Fig. 15 presents the variation in the three resistance forces across the different vehicles as determined by each vehicle's specifications.

Considering the different fuel types, diesel was observed to be more fuel efficient than gasoline, as demonstrated by a comparison between Astra and Urvan vehicles, which are typically manufactured in either gasoline or diesel versions [64]. Fuel consumption and CO_2 emissions for the diesel-powered Astra under rainfall conditions were 2.77 l/100 km and 7.36 $kgCO_2eq$, respectively, representing a 16.3 % reduction compared to the gasoline-powered Astra. In contrast, the gasoline-powered Urvan exhibited fuel consumption and CO_2 emissions of 9.45 l/100 km and 21.2 $kgCO_2eq$, respectively, which is 19.26 % higher than the diesel-powered Urvan. Similar findings were reported in studies by [65,66], which identified lower fuel consumption and CO_2 emissions in diesel vehicles compared to the corresponding gasoline-powered vehicles. The superior fuel efficiency associated with diesel vehicles is attributable to the higher energy content of diesel fuel. According to [67], diesel contains approximately 11 % more energy per volume basis compared to gasoline.

Impacts of weather intensity

The rate of impacts from the weather factors depended on the intensity variations across the months. According to [17], intensity is a critical factor in weather-induced vehicle fuel consumption and emissions. An increase in rainfall from 0.4 mm in January to 5.8 mm in June resulted in a 5 % rise in fuel consumption/emissions. Additionally, a 7.5 % increase was observed when wind speed rose from 6.5 m/s in January to 9.8 m/s in August under headwind, while tailwind led to a 0.2 % decrease. Consequently, every 1 mm increase in rainfall results in approximately 1 % rise in fuel consumption /emissions, whereas every 1 m/s increase in headwind leads to 2.3 % rise in emissions. In contrast, tailwind conditions yield a 0.06 % decrease per 1 m/s increase. Fig. 14 depicts the percentage changes in fuel consumption/emissions across the different months based on corresponding weather factors. Similarly, [68] observed significant impacts of higher precipitation on fuel consumption of limestone and clay trucks. Using average monthly precipitation data in Turkey, the highest fuel consumption was recorded in April, the month with the highest precipitation, while July, the driest month, exhibited the lowest fuel consumption. Additionally, [69] reported an increasing trend in fuel consumption as rain intensity increased, with average fuel consumption during heavy rainfall being 53 % greater than under dry weather conditions. Furthermore, [20] identified a linear relationship between wind speed and fuel consumption, where increasing wind intensity resulted in significant increments in fuel consumption for gasoline-powered vehicles.

Quantification of combined rainfall and wind effects

According to [17,70], the combined effects of rainfall and headwind induce complex vehicle flow patterns, resulting in significant changes in aerodynamic forces and consequently, fuel consumption and emissions. Fig. 16 illustrates the relationship between the

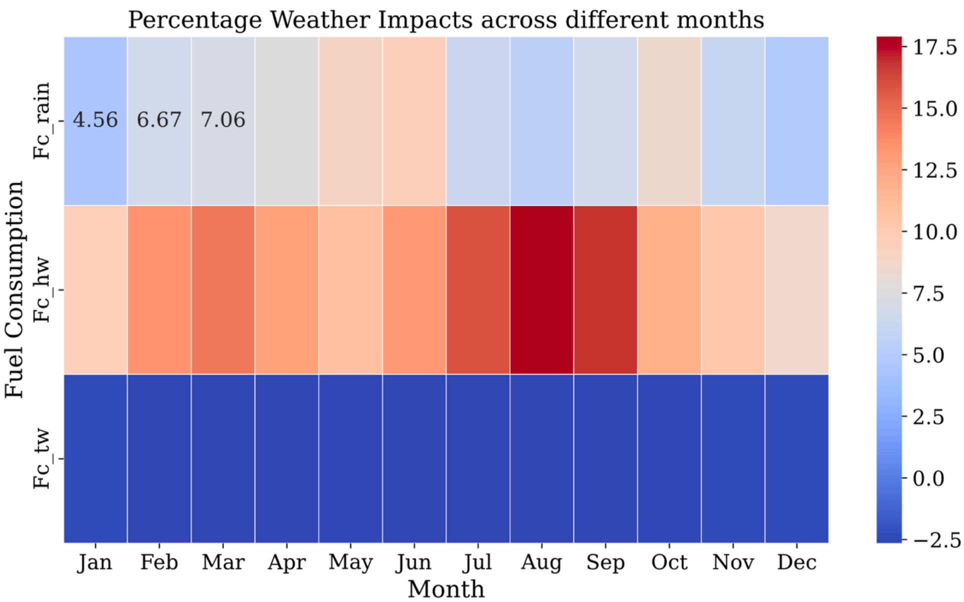

Fig. 14. Monthly fuel consumption changes based on weather intensity.

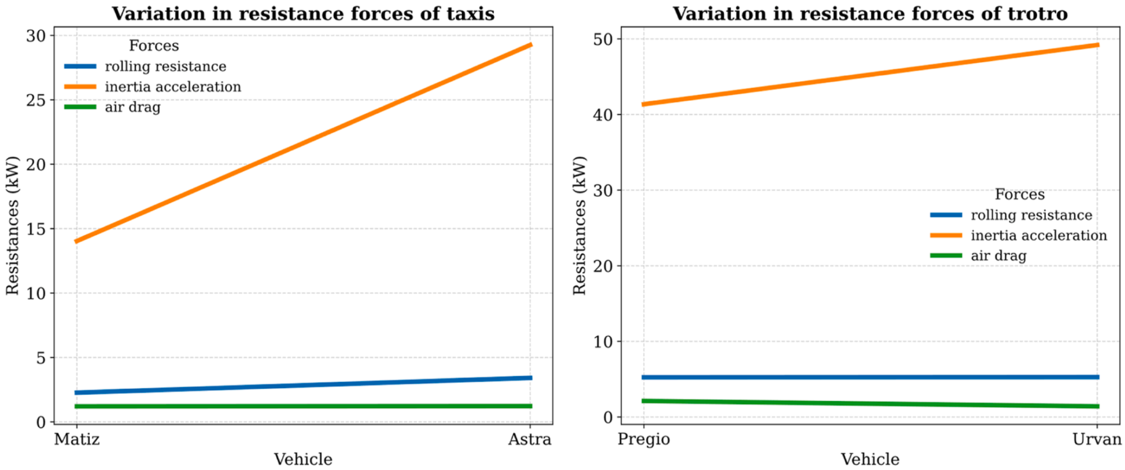

Fig. 15. Resistance forces for different vehicles based on specifications.

interactive (rain-headwind) and individual effects. Aerodynamic drag from the combined interaction was 2 to 4.5 times greater than drag caused by rainfall alone, and 1.5 to 6 times greater than drag due to headwinds, varying across the months. In terms of fuel consumption and emissions, the combined effects were 10 % to 37 % higher compared to rainfall alone effects, and 5 % to 66 % higher relative to headwind impacts, depending on monthly intensity levels. Similarly, [54] observed a substantial rise in impacts when both factors were combined, compared to the individual effects of rainfall and wind.

Model validation results

Results from the error analysis, based on the comparison between observed data and model predictions, are presented in Table 2. The R^2 values indicate that the combined model explained a greater proportion of the variability in fuel consumption compared to the individual models. However, the mean absolute percentage error (MAPE) for the combined model was slightly higher, likely due to increased model complexity. Overall, the obtained R^2 values indicate a good fit between the proposed models and the observed data, while the MAE and MAPE values reflect lower levels of absolute and percentage prediction errors, particularly in the individual rainfall and wind models.

Table 3 displays the results of the sensitivity analysis. Standardized regression coefficient (SRC) values illustrate a strong positive linear relationship between the weather factors and fuel consumption, indicating high sensitivity of the model output to variations in rainfall and wind speed. The minimal variation in the margin of error and narrow confidence intervals suggest that the estimated impact of the weather factors on fuel consumption is precise and accurate.

Based on the experimental and sensitivity analysis results, the models can be described as robust and consistent, highlighting the reliability of the findings and establishing the suitability of the models for practical applications such as offline fuel estimation prior to a journey.

Conclusion

The study modified a physics-based model by [31] to quantify the effects of rainfall and wind on four automobiles- Matiz, Astra, Pregio and Urvan. The model, which primarily centers on engine power and vehicle physical specifications, was enhanced by integrating weather factors as the main predictor variables, representing an advancement over conventional single-dimension physical models [23]. Rainfall data obtained from the Ghana Meteorological Agency were converted into terminal velocity using the Atlas and Ulbrich (1977) model. Wind speed data were further quantified based on the longitudinal direction of wind - headwind and tailwind. Both weather factors significantly influenced aerodynamic resistance and, ultimately, fuel consumption and emissions. Rainfall and headwind conditions increased drag by 0.8 to 1.7 kW and 1.5 to 3 kW, respectively, while tailwind reduced drag by up to 0.4 kW across the months. Consequently, fuel consumption and CO_2 emissions rose by 5 % as rainfall increased from 0.44 mm to 5.84 mm, while increasing wind speed from 6.53 m/s to 9.79 m/s resulted in a 7.5 % increase under headwind conditions and a 0.2 % reduction under tailwind conditions.

The model demonstrated robustness and effectiveness, as validated through field experiments and sensitivity analysis, thereby strengthening the reliability of the findings. To the authors' knowledge, the study has provided the first robust empirical data on the impacts of rainfall and wind on vehicle fuel consumption in Ghana, offering a valuable blueprint for future research.

Overall, the study presents two main contributions to the literature: the first empirical assessment of weather impacts on fuel consumption and emissions in Ghana; and the advancement of physical vehicle modeling through the integration of weather variables, enabling more realistic estimates under varying environmental conditions.

Further research should incorporate crosswinds and precipitation-induced road surface conditions to build upon the already

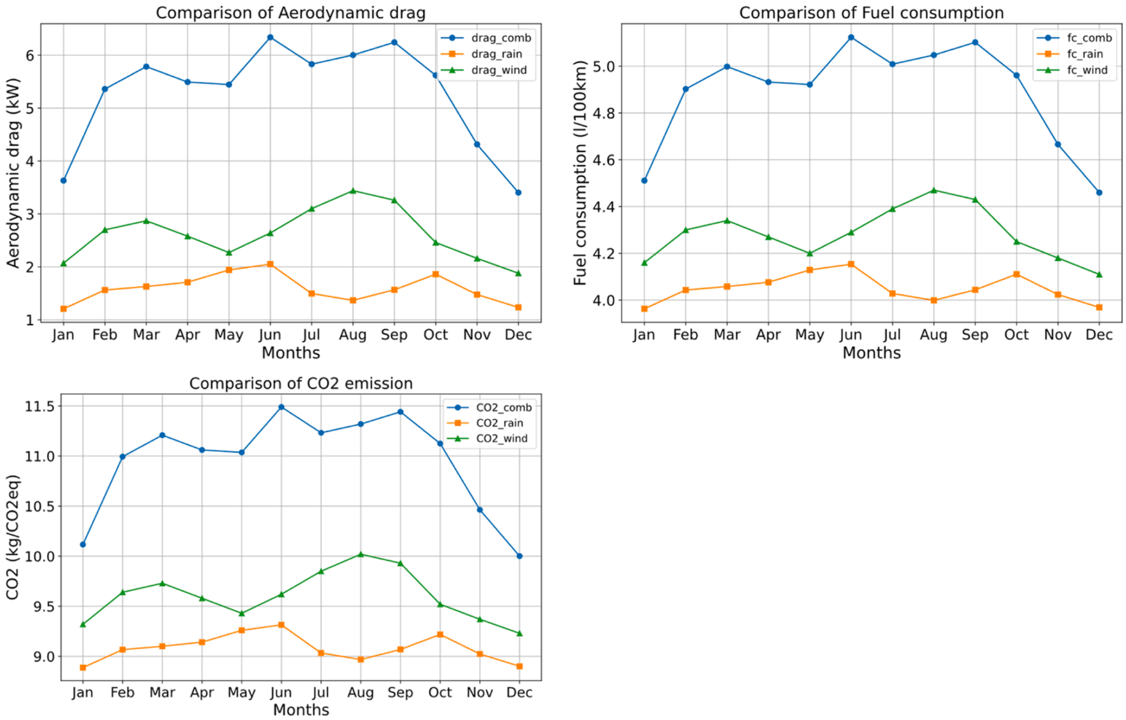

Fig. 16. Effects of rain-wind interactions.

Table 2
Field error analysis results.

Weather factors	R^2	MAE	MAPE
Rain	0.83	0.28	10.44
Wind	0.86	0.67	10.64
Rain + wind	0.88	0.39	15.45

Table 3
Uncertainty analysis results.

Error Analysis	Rainfall	Wind speed
Mean	3.6761	7.1851
Margin of error	0.0543	1.59
Confidence Interval	3.6218 -3.7304	5.59 -8.78
Standardized Regression coefficient	0.985	0.957

captured aerodynamic effects of rainfall, as well as headwind and tailwind influences. Inclusion of the additional factors will support the development of a multi-dimensional weather-based vehicle model, facilitating a more comprehensive analysis of wind and rainfall impacts on fuel consumption and emissions.

Policy implications

The study reveals a vicious cycle between road transport and climate change, where intensified climatic variations contribute to increased fuel consumption and emissions, further exacerbating climate change. Consequently, national and regional transport authorities must integrate weather-related impacts on road transport emissions into policy frameworks to support the development of climate-resilient transport system. To facilitate effective integration, policy measures should include capacity-building initiatives aimed at promoting the adoption of fuel-efficient aerodynamic add-on devices, such as vortex generators, wind and rain deflectors, which improve fuel efficiency and reduce emissions by minimizing aerodynamic resistance forces, as evidenced by studies such as [59, 71]. The capacity-building initiatives should encompass technical training and sensitization programs that highlight the application, performance and operational benefits of aerodynamic devices.

Additionally, collaborative engagement among academic institutions, transport authorities and other relevant stakeholders should be encouraged to ensure the efficient execution of comprehensive projects that quantify the annual contributions of seasonal weather variations to the total greenhouse gas emissions from the transport sector. Such projects should include all registered vehicles nationwide to broaden the scope of assessment and support the development of robust, climate-resilient strategies.

Furthermore, long-term mitigation of climate change requires a reduction in fossil fuel dependency. Prioritizing the adoption of alternative fuels through fiscal incentives, such as tax reductions on liquefied petroleum gas (LPG), the currently predominant alternative fuel, can stimulate consumer demand for cleaner fuel options over conventional fuels, thereby supporting the national target of achieving net-zero emissions by 2060 [72].

Data availability data

Will be made available on request.

Funding

Study was financially supported by West African Science Service Centre on Climate Change and Adapted Land Use (WASCAL).

CRediT authorship contribution statement

Janet Appiah Osei: Conceptualization, Methodology, Formal Analysis, Writing-Original Draft, Writing- review & editing. **Rabani Adamou**: Supervision, Writing- review & editing. **Amos T. Kabo-Bah**: Supervision, Writing- review & editing. **Satyanarayana Narra**: Supervision, Writing- review & editing, **Konin Pierre-Claver Kakou**: Visualization, Writing- review & editing.

Declaration of competing interest

The authors declare that they have no known competing financial interests or personal relationships that could have appeared to influence the work reported in this paper.

References

[1] Ardayfio-Schandorf, E., Yankson, P. W. K., & Bertrand, M. G. The mobile city of Accra: urban families, housing and residential practices= Accra, capitale en mouvement: familles citadines, logement et pratiques résidentielle.

[2] C.S. Wemegah, E.I. Yamba, J.N. Aryee, F. Sam, L.K. Amekudzi, Assessment of urban heat island warming in the greater accra region, Sci. Afr. 8 (2020) e00426.

[3] C. Fagariba, S. Song, Assessment of impediments and factors affecting waste management: A case of Accra Metropolis Montmorillonite Nanosheets View project solid/liquid interface interactions characterization using AFM View project, Acad. J. Environ. Sci. (December) (2016), https://doi.org/10.15413/ajes.2016.0125.

[4] M. Padi, B.A.K. Foli, E.S. Nyadjro, K. Owusu, G. Wiafe, Extreme rainfall events over Accra, Ghana, in recent years, Remote Sens. Earth Syst. Sci. 5 (1–2) (2022) 71–82, https://doi.org/10.1007/s41976-021-00062-1.

[5] B. Kashi, S. Carello, Urban transport Solutions for Accra. www.copenhagenconsensus.com, 2020.

[6] M.H. Andreasen, J. Agergaard, L. Møller-Jensen, M. Oteng-Ababio, G.A.B. Yiran, Mobility disruptions in Accra: recurrent flooding, fragile infrastructure and climate change, Sustain 14 (21) (2022) 1–19, https://doi.org/10.3390/su142113790.

[7] J.A. Osei, R. Adamou, A.T. Kabo-Bah, S. Narra, Climate variability and change impacts on vehicular fuel consumption and emissions- A systematic overview in Africa, STED J. 5 (1) (2023) 50–77.

[8] M. Zhou, H. Jin, W. Wang, A review of vehicle fuel consumption models to evaluate eco-driving and eco routing, Transp. Res. D 49 (2016) 203–218, https://doi.org/10.1016/j.trd.2016.09.0081361-9209.

[9] E.T. Mansur, R. Mendelsohn, W. Morrison, Climate change adaptation: A study of fuel choice and consumption in the US energy sector, J. Environ. Econ. Manag. 55 (2) (2008) 175–193.

[10] K. Tadic, D. Glavic, The analysis of fuel consumption models: A review and assessment, Put Saob. 65 (1) (2019) 19–23, https://doi.org/10.31075/pis.65.01.03.

[11] P.A. Kwakwa, G. A, O.-F.K Anthony, A time series analysis of fossil fuel consumption in Sub-Saharan Africa : evidence from Ghana, Kenya and South Africa, Int. J. Sustain. Energy Plan. Manag. 17 (2018) 31–44.

[12] J. Mensah, J. Annan, F. Andoh-baidoo, Assessing the impact of vehicular traffic on energy demand in Accra Metropoli, J. Manag. Policy Pract. 15 (4) (2014) 127–136.

[13] B. Musah, L. Peng, Y. Xu, Urban congestion and pollution: A quest for cogent solutions for Accra City, IOP Conf. Ser.: Earth Environ. Sci. 435 (1) (2020), https://doi.org/10.1088/1755-1315/435/1/012026.

[14] N.L.H. Hien, A.L. Kor, Analysis and prediction model of fuel consumption and carbon dioxide emissions of light-duty vehicles, Appl. Sci. 12 (2022) 803, https://doi.org/10.3390/app12020.

[15] b S. Mehrotra, B. Lefevre, R. Zimmerman, H. Gerçek, K. Jacob, S. Srinivasan, Climate change and urban transportation systems. Climate Change and Cities: first assessment report of the Urban Climate Change Research Network, in: C. Rosenzweig, W.D. Solecki, S.A. Hammer, S. Mehrotra (Eds.), Cambridge University Press, Cambridge, UK, 2011, pp. 145–177.

[16] D. Choi, M. Beardsley, D. Brzezinski, J. Koupal, J. Warila, MOVES sensitivity analysis: the impacts of temperature and humidity on emissions, in: US EPA–Proceedings from the 19th Annual International Emission Inventory Conference, 2010, pp. 1–15. https://www3.epa.gov/ttnchie1/conference/ei19/session6/choi.pdf.

[17] W.Y. Pao, M. Carvalho, F. Hosseinnouri, L. Li, C. Rouaix, M. Agelin-Chaab, H. Hangan, I. Gultepe, J. Komar, Evaluating weather impact on vehicles: a systematic review of perceived precipitation dynamics and testing methodologies, Eng. Res. Express 6 (1) (2024), https://doi.org/10.1088/2631-8695/ad2033.

[18] R. Shang, Y. Zhang, Z.J. Max Shen, Y. Zhang, Analyzing the effects of road type and rainy weather on fuel consumption and emissions: A mesoscopic model based on big traffic data, IEEE Access 9 (2021) 62298–62315, https://doi.org/10.1109/ACCESS.2021.3074303.

[19] N.G. Zacharof, G. Fontaras, B. Ciuffo, S. Tsiakmakis, K. Anagnostopoulos, A. Marotta, J. Pavlovic, Review of in use factors affecting the fuel consumption and CO_2 emissions of passenger cars, Publications Office of the European Union, Luxembourg, 2016, https://doi.org/10.2790/74318.

[20] Y. Yang, N. Gong, K. Xie, Q. Liu, Predicting gasoline vehicle fuel consumption in energy and environmental impact based on machine learning and multidimensional big data, Energies 15 (2022) 1602.

[21] M.N. Sudin, M.A. Abdullah, S.A. Shamsuddin, F.R. Ramli, M.M. Tahir, Review of research on vehicles aerodynamic drag reduction methods, Int. J. Mech. Mechatron. Eng. 14 (2) (2014) 35–47.

[22] B. Predić, M. Madić, M. Roganović, D. Karabašević, D. Stanujkić, Implementation of computationally efficient Taguchi robust design procedure for development of ANN fuel consumption prediction models, Transport 33 (3) (2018) 751–764, https://doi.org/10.3846/transport.2018.5174.

[23] D. Zhao, H. Li, J. Hou, P. Gong, Y. Zhong, W. He, Z. Fu, A review of the data-driven prediction method of vehicle fuel consumption, Energies 16 (14) (2023), https://doi.org/10.3390/en16145258.

[24] M.K. Habib, S.A. Ayankoso, F. Nagata, Data-driven modeling: concept, techniques, challenges and a case study, in: 2021 IEEE International Conference on Mechatronics and Automation, ICMA 2021, 2021, pp. 1000–1007, https://doi.org/10.1109/ICMA52036.2021.9512658. *August*.

[25] M. Ehsani, A. Ahmadi, D. Fadai, Modeling of vehicle fuel consumption and carbon dioxide emission in road transport, Renew. Sustain. Energy rev. 53 (2016) 1638–1648, https://doi.org/10.1016/j.rser.2015.08.062.

[26] H. Wang, X. Ou, X. Zhang, Mode, technology, energy consumption, and resulting CO_2 emissions in China's transport sector up to 2050, Energy Policy 109 (2017) 719–733, https://doi.org/10.1016/j.enpol.2017.07.010.

[27] B. Ovai, A.P.H. Kunadu, N. Gake, C. Doku, R.Y. Otwey, Food safety risk factors associated with chicken consumption and chicken handling practices in Accra, Ghana, Sci. Afr. 16 (2022) e01263.

[28] Ghana Statistical Service (2014). 2010 Population and Housing Census. District analytical Report Accra Metropolitan.

[29] C. Amoako, E.F. Boamah, The three-dimensional causes of flooding in Accra, Ghana, Int. J. Urban Sustain. Dev. 7 (1) (2015) 109–129, https://doi.org/10.1080/19463138.2014.984720.

[30] E.F. Redish, K.A. Smith, Looking beyond content, J. Eng. Educ. (2008) 295–307.

[31] M. Ben-Chaim, E. Shmerling, A. Kuperman, Analytic modeling of vehicle fuel consumption, Energies 6 (1) (2013) 117–127, https://doi.org/10.3390/en6010117.

[32] K. Das, S. Sharma, Eco-routing navigation systems in electric vehicles: A comprehensive survey. Autonomous and Connected Heavy Vehicle Technology, Elsevier Inc, 2022, https://doi.org/10.1016/B978-0-323-90592-3.00006-9.

[33] S. Sebben, T. Walker, C. Landström, Fundamentals, basic principles in road vehicle aerodynamics and design, Encycl. Automot. Eng. 1 (2014) 1–16, https://doi.org/10.1002/9781118354179.auto241.

[34] Wood, R. M. (2004). Impact of advanced aerodynamic technology on transportation energy consumption. *SAE Technical Papers, 2004*(724). https://doi.org/10.4271/2004-01-1306.

[35] M. Askerdal, J. Fredriksson, L. Laine, Development of simplified air drag models including crosswinds for commercial heavy vehicle combinations, Veh. Syst. 62 (5) (2024) 1085–1102, https://doi.org/10.1080/00423114.2023.2213786.

[36] Tulpule, P., Marano, V., & Rizzoni, G. (2011). Effect of traffic, road and weather information on PHEV energy management (No. 2011-24-0162). SAE Technical Paper.

[37] S. Kobayashi, S. Plotkin, S.K. Ribeiro, Energy efficiency technologies for road vehicles, Energy Effic. 2 (2) (2009) 125–137, https://doi.org/10.1007/s12053-008-9037-3.

[38] J. Jerrelind, P. Allen, P. Gruber, M. Berg, L. Drugge, Contributions of vehicle dynamics to the energy efficient operation of road and rail vehicles, Veh. Syst. Dyn. 59 (7) (2021) 1114–1147, https://doi.org/10.1080/00423114.2021.1913194.

[39] S. Hasselwander, A. Galich, S. Nieland, Impact of climate change on the energy consumption of passenger car vehicles, World Electr. Veh. J. 13 (8) (2022), https://doi.org/10.3390/wevj13080146.

[40] T. Wu, X. Han, M.M. Zheng, X. Ou, H. Sun, X. Zhang, Impact factors of the real-world fuel consumption rate of light duty vehicles in China, Energy 190 (2020) 116388, https://doi.org/10.1016/j.energy.2019.116388.

[41] W.L. Snowsill, Particle sizing, in: W. Boyes (Ed.), Instrumentation reference book, 4th ed., Butterworth-Heinemann, 2010, pp. 175–189, https://doi.org/10.1016/B978-0-7506-8308-1.00016-4.

[42] M.A. Serio, F.G. Carollo, V. Ferro, Raindrop size distribution and terminal velocity for rainfall erosivity studies. A review, J. Hydrol. (2019) (2019), https://doi.org/10.1016/j.jhydrol.2019.06.040.

[43] K. Loftus, R.D. Wordsworth, The physics of falling raindrops in diverse planetary atmospheres, J. Geophys. Res.: Planets 126 (4) (2021), https://doi.org/10.1029/2020JE006653.

[44] A.C. Best, Empirical formulae for the terminal velocity of water drops falling through the atmosphere, Q. J. R. Meteorol. Soc. 76 (1950) 302–311.

[45] E. Kessler, On the distribution and continuity of water substance in atmospheric circulations, Meteorological Monographs series, 32, American Meteorological Society, Boston, USA, 1969, p. 84.

[46] D. Atlas, R.C. Srivastava, R.S. Sekhon, Doppler radar characteristics of precipitation at vertical incidence, Rev. Geophys. 11 (1973) 1–35.

[47] D. Atlas, C.W. Ulbrich, Path and area-integrated rainfall measurement by microwave attenuation in the 1–3cm band, J. Appl. Meteorol. 16 (1977) 1322–1331.

[48] P.T. Willis, Functional fits to some observed drop size distributions and parameterization of rain, J. Atmos. Sci. 41 (9) (1984) 1648–1661.

[49] E.A. Brandes, G. Zhang, J. Vivekanandan, Experiments in rainfall estimation with a polarimetric radar in a subtropical environment, J. Appl. Meteorol. 41 (2002) 674–685.

[50] A.T. Zachiotis, E.G. Giakoumis, Monte Carlo simulation methodology to assess the impact of ambient wind on emissions from a light-commercial vehicle running on the worldwide harmonized light-duty vehicles test cycle (WLTC), Energies 14 (3) (2021) 661, https://doi.org/10.3390/en14030661.

[51] X. Nie, C. Min, Y. Pan, Z. Li, G. Królczyk, An improved deep neural network model of intelligent vehicle dynamics via linear decreasing weight particle swarm and invasive weed optimization algorithms, Sensors 22 (13) (2022), https://doi.org/10.3390/s22134676.

[52] D. Chicco, M.J. Warrens, G. Jurman, The coefficient of determination R-squared is more informative than SMAPE, MAE, MAPE, MSE and RMSE in regression analysis evaluation, PeerJ Comput. Sci. 7 (2021) 1–24, https://doi.org/10.7717/PEERJ-CS.623.

[53] A. Garg, K. Kazunari, T. Pulles, IPCC Guidelines for National greenhouse gas inventories. http://www.ghgprotocol.org/includes/getTarget.asp?type=d&id=MTYwNjQ, 2006.

[54] W.Y. Pao, L. Li, M. Agelin-Chaab, Wind-driven rain effects on automotive camera and LiDAR performances, in: Paper presented at the Canadian Society for Mechanical Engineering (CSME) International Congress 2022, Edmonton, Alberta, 2022, https://doi.org/10.7939/r3-e4xk-g069.

[55] H. Almér, Machine learning and statistical analysis in fuel consumption prediction for heavy vehicles. A doctoral dissertation, KTH Royal Institute of Technology, Sweden, 2015.

[56] Raeesi, A., McAuliffe, B., & Galler, J. (2023). Impact of precipitation drag on a road vehicle (No. 2023-01-0792). SAE Technical Paper. https://doi.org/10.4271/2023-01-0792.

[57] M. Carvalho, H. Hangan, Modelling weather precipitation intensity on surfaces in motion with application to autonomous vehicles, Sensors 23 (19) (2023), https://doi.org/10.3390/s23198034.

[58] W. Ren, J. Reutzsch, B. Weigand, Direct numerical simulation of water droplets in turbulent flow, Fluids 5 (3) (2020), https://doi.org/10.3390/fluids5030158.

[59] D.S. Nath, P.C. Pujari, A. Jain, V. Rastogi, Drag reduction by application of aerodynamic devices in a race car, Adv. Aerodyn. 3 (1) (2021), https://doi.org/10.1186/s42774-020-00054-7.

[60] M.Z. Abedin, A.N.M.M.I Mukut, Review on aerodynamic drag reduction of vehicles, Int. J. Eng. Mater. Manuf. 4 (1) (2019) 1–14, https://doi.org/10.26776/ijemm.04.01.2019.01.

[61] S. Alshayeb, A. Stevanovic, J.R. Effinger, Investigating impacts of various operational conditions on fuel consumption and stop penalty at signalized intersections, Int. J. Transp. Sci. Technol. 11 (4) (2022) 690–710, https://doi.org/10.1016/j.ijtst.2021.09.005.

[62] Anttila, P., Nummelin, T., Kari, V., Laitila, J., & Ala-ilom, J. (2022). Transportation Research Interdisciplinary Perspectives effect of vehicle properties and driving environment on fuel consumption and CO2 emissions of timber trucking based on data from fleet management system. 15, 0–3. https://doi.org/10.1016/j.trip.2022.100671.

[63] C.A. Romero, P. Correa, E.A. Ariza Echeverri, D. Vergara, Strategies for reducing automobile fuel consumption, Appl. Sci. 14 (2) (2024) 1–27, https://doi.org/10.3390/app14020910.
[64] J.A. Osei, R. Adamou, A.T. Kabo-Bah, S. Narra, Assessment of commercial vehicle models in the urban public transport of Ghana, Discov Cities 2 (2025) 36, https://doi.org/10.1007/s44327-025-00081-3.
[65] M. Opetnik, S. Hausberger, C.U. Matzer, S. Lipp, L. Landl, K. Weller, M. Elser, The impact of vehicle technology, size class, and driving style on the ghg and pollutant emissions of passenger cars, Energies 17 (9) (2024) 2052.
[66] S.O. Ismaila, B.O. Bolaji, O.R. Adetunji, N.O. Adekunle, T.A. Yusuf, H.O. Sanusi, On vehicular emissions of petrol and diesel engines, Ann. Fac. Eng. Hunedoara 11 (3) (2013) 177.
[67] C.J. Cleveland, C.G. Morris (Eds.), Dictionary of energy, 2nd ed., Elsevier, 2014, pp. 217–246, https://doi.org/10.1016/B978-0-08-096811-7.50006-8.
[68] O. Golbasi, E. Kina, Haul truck fuel consumption modeling under random operating conditions: A case study, Transp. Res. D: Transp. Environ. 102 (2022) 103135, https://doi.org/10.1016/j.trd.2021.103135.
[69] M.V. Faria, P.C. Baptista, T.L. Farias, J.M.S. Pereira, Assessing the impacts of ambient environment on driving behavior patterns, Transportation 47 (3) (2020) 1311–1337, https://doi.org/10.1007/s11116-018-9965-5.
[70] M. Yu, X. Sheng, J. Liu, W. Huo, M. Li, Effects of wind-rain coupling on the aerodynamic characteristics of a high-speed train, J. Wind Eng. Ind. Aerodyn. 231 (2022) 105213, https://doi.org/10.1016/j.jweia.2022.105213.
[71] S.C.V. Ramana Murty Naidu, V.M. Madhavan, S. Chinta, R. Manikandan, A. Premkumar, R. Girimurugan, Analysis of aerodynamic characteristics of car diffuser for dissimilar diffuser angles on Sedan's using CFD, Mater. Today: Proc. 92 (2023) 240–248, https://doi.org/10.1016/j.matpr.2023.04.379.
[72] J.A. Osei, R. Adamou, A.T. Kabo-Bah, S. Narra, Decarbonisation in the transport sector of Ghana using autogas, in: Advances in Science and Technology (Vol. 160, pp.267–278). *Africa International Conference on Clean Energy and Energy Storage*, Trans Tech Publications Ltd., 2025, https://doi.org/10.4028/p-ezf4lf.